

POST-BIFURCATION OF PERFECT AND IMPERFECT SPHERICAL ELASTIC MEMBRANES

D. M. HAUGHTON

School of Mathematics, University of Bath, Claverton Down, Bath, BA2 7AY, England

(Received 19 October 1979; in revised form 30 January 1980)

Abstract—When a spherical elastic membrane is inflated it is well known that it may bifurcate into an aspherical mode after the pressure maximum is reached. Upon further inflation the spherical configuration is regained. Here we follow the developing aspherical solution path, for specific forms of strain-energy function, using a simple numerical method. For a realistic strain-energy function it is shown that the post-bifurcation solution curve connects the two bifurcation points. We also consider the inflation of imperfect spherical membranes and show that bifurcation may still occur. For the class of Ogden materials we investigate the asymptotic shape of arbitrary axisymmetric membranes.

1. INTRODUCTION

The initiation of aspherical modes during the inflation of spherical membranes has been considered by several authors[1-3] for example. Most recently Haughton and Ogden[4, 5] have considered the problem in terms of a general (incompressible, isotropic) hyperelastic material. In particular, it was shown that all bifurcation points occur (if at all) between the maximum and minimum values of the inflating pressure. Also, for realistic material models which exhibit both a pressure maximum and minimum, it was shown that the bifurcation points must occur in pairs. This leads to the natural conjecture that the first bifurcation point to occur indicates the initiation of the aspherical mode, while the second bifurcation point (of the same mode number) indicates the return to the spherical configuration. Sewell[6] had previously made this conjecture on the basis of experimental results[7].

Needleman[3] has considered the inflation of *slightly imperfect* spherical membranes. His results indicate that a perfectly spherical membrane is likely to show a "closed loop" behaviour. That is, an aspherical solution path connecting the two bifurcation points, at least for certain specific forms of strain-energy function.

In the bifurcation analysis of inflated spherical shells it is supposed that the deformation away from the spherical configuration is *small*. This means that it is not possible to consider the developing aspherical paths.

In this paper we first formulate the equations governing the axisymmetric inflation of an initially axisymmetric membrane. These equations, in different forms, are well known. However, the derivation of the equations allows us to introduce the relevant notation and to put this work into the context of the previous work involving bifurcation points only[4, 5].

In Section 4 we suppose that the membrane is initially perfectly spherical. The resulting system of ordinary differential equations (containing the inflating pressure as a parameter) are then solved numerically for specific forms of strain-energy function. The resulting post-bifurcation curves are plotted to show how the *deformation* differs from that in the spherical configuration, and also to show the developing aspherical *shape* of the membrane.

In Section 5 we consider spherical membranes with thickness imperfections. The resulting solution curves are compared with the post-bifurcation curves for the perfectly spherical case. It is shown that the bifurcation points may be retained or destroyed depending on the form of the imperfection. This particular feature of imperfect membranes was not considered in [3].

Certain forms of strain-energy function do not show the "closed loop" post-bifurcation behaviour and so the asymptotic shape of the membrane (as the enclosed volume $\rightarrow \infty$) is of some interest. In Section 6 we consider the asymptotic shape of inflated axisymmetric membranes for the class of Ogden materials[8]. This follows the analysis of Isaacson[9] who considered the case of a Mooney-Rivlin strain-energy function. We show that the class of strain-energy functions considered can be divided into two subclasses. In one the asymptotic shape of the membrane is necessarily spherical, independently of its initial shape or

thickness variations, while in the second we cannot, at present, rule out the possibility of aspherical asymptotic shapes even for initially spherical membranes.

2. MEMBRANE EQUATIONS

Let the middle surface of the membrane in its undeformed (and unstressed) configuration be specified by the *cylindrical coordinates* (R, Φ, Z) , where the Z -axis coincides with the assumed axis of rotational symmetry. Any point on the middle surface can be defined by the arc length S and the angle Φ , where $R = R(S)$, $Z = Z(S)$. For a closed membrane we have

$$R(0) = R(L) = 0, \quad (1)$$

with

$$R(S) > 0 \quad S \in (0, L), \quad (2)$$

where L is the total meridional arc length of the membrane. The material of the membrane is completely specified by defining the undeformed thickness $H(S)$. We make the usual membrane assumption that

$$H_{\max}/\kappa_{\min} \ll 1, \quad (3)$$

where H_{\max} is the maximum thickness of the membrane and κ_{\min} is the minimum radius of curvature of the middle surface.

The middle surface of the membrane, together with the inner and outer surfaces, are assumed to be smooth. Combined with the rotational symmetry, this leads to

$$H'(0) = H'(L) = 0, \quad (4)$$

$$Z'(0) = Z'(L) = 0, \quad (5)$$

where the prime denotes d/dS .

Now suppose that the membrane is deformed into the "current" configuration by the application of an inflating pressure $P > 0$ to the inner surface. The points on the new middle surface are defined by the cylindrical coordinates $(r(S), \phi, z(S))$.

From the rotational symmetry we have $\phi = \Phi$. Since the membrane remains closed and the deformation is smooth eqns (1), (2), (4) and (5) are valid for $r(S)$, $z(S)$ and $h(S)$, where $h(S)$ is the thickness of the membrane in the current configuration.

The principal axes of the deformation are in the meridional, longitudinal and normal directions. The corresponding principal stretches, evaluated on the middle surface, are given by

$$\lambda_1 = [(r')^2 + (z')^2]^{1/2}, \quad (6)$$

$$\lambda_2 = r/R, \quad (7)$$

and, because of the assumed incompressibility

$$\lambda_3 = (\lambda_1 \lambda_2)^{-1}. \quad (8)$$

We note that (7) is not valid at the poles of the membrane. However, it is easily shown that

$$\lambda_2 = \lambda_1 = |r'|, \quad S = 0, L. \quad (9)$$

From [4], or for a more detailed account [10], the equations of equilibrium can be written

$$r(h\sigma_{11})' + hr'(\sigma_{11} - \sigma_{22}) = 0, \quad (10)$$

$$z' \sigma_{22}/r \lambda_1 + \sigma_{11}(r'z'' - r''z')/\lambda_1^3 = \lambda_1 \lambda_2 P^*, \quad (11)$$

where $P^* = P/H(S)$ and σ_{11}, σ_{22} are the principal Cauchy stresses. Strictly, these stresses, and the quantities defined below, are all *averaged through the current thickness of the membrane*. See [4, 5] for details. However, for our purposes here, it is not necessary to consider this as the errors involved do not invalidate (10) or (11).

We note that the third equilibrium equation is identically satisfied, a consequence of the rotational symmetry.

Equations equivalent to (10) and (11) are well known, [9] and [11] for example.

If we assume the existence of a strain-energy function $W(\lambda_1, \lambda_2, \lambda_3)$ per unit volume, then we may write

$$\sigma_{11} = \lambda_1 \hat{W}_1, \quad \sigma_{22} = \lambda_2 \hat{W}_2, \tag{12}$$

where $\hat{W}(\lambda_1, \lambda_2) \equiv W(\lambda_1, \lambda_2, (\lambda_1 \lambda_2)^{-1})$ and $\hat{W}_\mu = \partial \hat{W} / \partial \lambda_\mu$ ($\mu = 1, 2$), having used the membrane approximation $\sigma_{33} = 0$. See [12] for details of a similar problem.

The boundary conditions necessary to complete the system are given by

$$r(0) = r(L) = z'(0) = z'(L) = 0. \tag{13}$$

We note that it is only the derivative of z that appears in (10), (11) and (13), hence the system is of third order and any one of (13) is surplus to requirements. It may be used, however, to speed convergence when we are solving the system numerically.

3. NUMERICAL METHOD

For the numerical examples given here we restrict attention to those membranes which initially have a spherical middle surface. We non-dimensionalize our coordinates by choosing the initial radius of the middle surface to be unity. If we now write θ for the (non-dimensionalized) arc length S , then

$$0 \leq \theta \leq \pi, \tag{14}$$

and

$$R = \sin \theta. \tag{15}$$

The strain-energy function \hat{W} and the pressure P are non-dimensionalized by choosing the ground state shear modulus to be unity.

As we have already mentioned, the system of eqns (10) and (11) is of third order. From (11), its derivative with respect to θ , and (10) it is possible to rewrite the equations as

$$r'' = \{ -r'[2z'\lambda_2' \hat{W}_{12} + \lambda_1(r'\lambda_2 + r\lambda_2' - r\lambda_2 H'/H)P^*] + \lambda_2(2\lambda_1 \hat{W}_1 - \lambda_2 \hat{W}_2) \times [(r')^2 \hat{W}_1 + (z')^2 \lambda_1 \hat{W}_{11}] P^* / (\hat{W}_1)^2 \} / (2z'\lambda_1 \hat{W}_{11}) \tag{16}$$

for $\theta \in (0, \pi)$,

$$z'' = \{ r'\lambda_2(\lambda_1 \hat{W}_{11} - \hat{W}_1)(\lambda_2 \hat{W}_2 - 2\lambda_1 \hat{W}_1)P^* / (\hat{W}_1)^2 - 2z'\lambda_2' \hat{W}_{12} - \lambda_1(r'\lambda_2 + r\lambda_2' - r\lambda_2 H'/H)P^* \} / (2\lambda_1 \hat{W}_{11}) \tag{17}$$

for $\theta \in [0, \pi]$, where the prime now denotes $d/d\theta$ and $\hat{W}_{11} = \partial^2 \hat{W} / \partial \lambda_1^2$, etc. having used (12).

From (7) we find that

$$\lambda_2' = 0 \quad \text{at} \quad \theta = 0, \pi. \tag{18}$$

Equations (9) and (18) with (4), (5), (11) and (17) enable us to show that

$$r''(0) = r''(\pi) = 0, \tag{19}$$

which completes the definition of the differential equations.

With the notation

$$\mathbf{x}^T = (r, r', z'), \quad (20)$$

we can write the equations of equilibrium as

$$\mathbf{x}' = \mathbf{f}(\mathbf{x}, P^*). \quad (21)$$

The pressure P^* appears in the equations as a parameter. In general it will be a given function of θ , but for the special case of a perfect spherical shell it will be constant.

Boundary conditions to complete the system are given by (any three of) (13).

When a particular form of strain-energy function has been specified and a particular pressure $P^*(\theta)$ is given then eqn (21) is solved numerically using a fourth-order Runge-Kutta method with Newton (secant) iteration. The solutions are calculated to four places of decimals. In none of the examples given here were any numerical difficulties encountered.

In considering slightly imperfect spherical membranes Needleman[3] used a completely different approach to arrive at the equilibrium equations and a different (numerical) method of solution to that used here.

4. POST-BIFURCATION OF SPHERICAL MEMBRANES

4.1 Spherical configuration and bifurcation points

In this section we restrict attention to membranes that are initially spherical with uniform thickness. Firstly, suppose that the spherical shape is maintained during inflation. We then have

$$\lambda_1 = \lambda_2 = \lambda \quad (\text{say}) \quad (22)$$

where λ is constant with respect to θ . The strain-energy function $\hat{W}(\lambda_1, \lambda_2)$ can be written $\hat{W}(\lambda) = \hat{W}(\lambda, \lambda)$, and we then have

$$P^* = \bar{W}_\lambda / \lambda^2, \quad (23)$$

where $\bar{W}_\lambda = \partial \hat{W} / \partial \lambda$. This follows from (11) after putting

$$r = \lambda \sin \theta, \quad z' = -\lambda \sin \theta, \quad (24)$$

for a spherical configuration, or alternatively see [5].

We note that eqn (10) is identically satisfied in the spherical configuration and so this corresponds to the "trivial" solution of the system.

It was also shown in [5] that bifurcations away from the trivial solution occur at turning points of the surface tension in the membrane. In our notation, these bifurcation points are given by solutions of

$$\lambda \bar{W}_{\lambda\lambda} - \bar{W}_\lambda = 0. \quad (25)$$

The values of λ satisfying (25) are the first (and last) possible bifurcation points to occur[5] and they correspond to the mode number $n = 1$.

For realistic forms of strain-energy function there will exist two values of λ satisfying (25), which must necessarily lie between the values of λ corresponding to the maximum and minimum values of the pressure P^* . There may be more (pairs of) bifurcation points lying between the turning points of the surface tension corresponding to higher order mode numbers.

4.2 Post-bifurcation

In order to give specific examples of post-bifurcation behaviour we restrict attention to the class of strain-energy functions proposed by Ogden[8]. In the present circumstances we can

write

$$\dot{W}(\lambda_1, \lambda_2) = \mu_n(\lambda_1^{\alpha_n} + \lambda_2^{\alpha_n} + (\lambda_1\lambda_2)^{-\alpha_n} - 3)/\alpha_n, \tag{26}$$

where the repetition of the index n implies summation over a finite number of terms. The material constants are such that

$$\mu_n\alpha_n > 0 \quad \text{each } n, \tag{27}$$

and we note that the ground state shear modulus μ is given by

$$\mu_n\alpha_n = 2\mu. \tag{28}$$

A three-term member of (26) which was shown in [8] to give good agreement with experimental data for a particular rubber-like material has parameters

$$\begin{aligned} \alpha_1 = 1.3, & \quad \alpha_2 = 5.0, & \quad \alpha_3 = -2.0, \\ \mu_1^* = 1.491, & \quad \mu_2^* = 0.003, & \quad \mu_3^* = -0.024, \end{aligned} \tag{29}$$

where $\mu_n^* = \mu_n/\mu$ are dimensionless.

The two (mode $n = 1$) bifurcation points for this strain-energy function are given by $\lambda = 1.772$ and 2.545 . Higher order modes are not possible.

To plot our results we choose λ (the principal stretch in the spherical configuration) as our abscissa. In this way λ may be thought of as our fundamental parameter defining a value of the pressure P^* through (23). The problem of stability when choosing the pressure as an (increasing) parameter is then avoided.

In order to plot a post-bifurcation curve we must define a measure of the ‘‘asphericity’’ which we denote by β . We first choose

$$\beta_1 = \max_{0 \leq \theta \leq \pi} \{|\lambda_1/\lambda - 1|, |\lambda_2/\lambda - 1|\}. \tag{30}$$

This then gives a measure of the difference in the deformation between the spherical and aspherical solutions. Note that $\beta_1 = 0$ if and only if the membrane is in the spherical configuration.

In Fig. 1 we plot β_1 against λ for the three-term strain-energy function (29). The ‘‘closed loop’’ behaviour is evident.

We recall that we have assumed *ab initio* that the aspherical solution path remains axisymmetric, which may not be the case in practice.

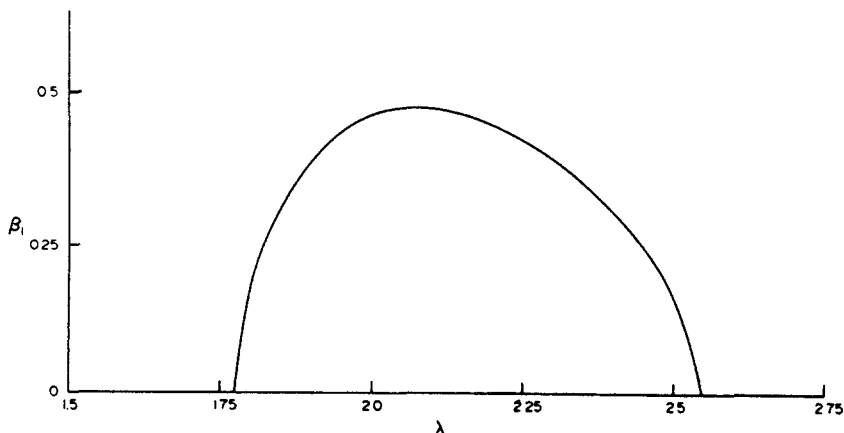


Fig. 1. Plot of the deformation asphericity β_1 against λ for the three-term strain-energy function (29).

It is well known that the deformation away from the spherical configuration (in the neighbourhood of the mode $n = 1$ bifurcation points) can either be through a thinning/thickening of the poles, or by a radial displacement asymmetric about the equatorial plane, or any combination of these. We find that the thinning/thickening is the dominant mode along the aspherical solution path with a small change of shape. Since we may have either pole thinning or thickening these two solutions are equivalent, the only difference between them is a rigid body rotation of π radians. We note that *both* of these solutions map onto the single aspherical solution path.

If, for definiteness, we suppose that $r'(0) = \lambda_1(0) = \lambda_2(0) > \lambda > |r'(\pi)| = \lambda_1(\pi) = \lambda_2(\pi)$ then, for the strain-energy function (29),

$$\beta_1 = r'(0)/\lambda - 1. \quad (31)$$

In order to demonstrate the *change in shape* of the membrane we choose a second asphericity parameter given by

$$\beta_2 = (\max_{0 \leq \theta \leq \pi} \{r^*\} - \min_{0 \leq \theta \leq \pi} \{r^*\})/\lambda \quad (32)$$

where

$$r^*(\theta) = (r^2 + z^2)^{1/2} \quad (33)$$

is the radius of the middle surface in *spherical coordinates*. In (33) we have taken

$$z(0) = -z(\pi). \quad (34)$$

In (32) we divide by λ in order to normalize the asphericity. Note that $\beta_2 = 0$ if and only if the shape of the membrane is spherical. In Fig. 2 we plot β_2 against λ for the three-term strain-energy function (29).

The small values of β_2 in Fig. 2 indicate the almost spherical shape of the membrane through the aspherical range, even though the deformation can be very different from that in the spherical configuration, as shown in Fig. 1. Following the post-bifurcation path we find that the initial aspherical deformation is composed largely of the thinning/thickening of the poles. The polar diameter is virtually maintained but there is some reduction in the equatorial diameter *when compared with the membrane in the spherical configuration at the same pressure*. This mode of behaviour is continued until the first local maximum in Fig. 2 is reached. The asphericity then declines, the equatorial radius growing back towards the values λ , (that it would have in the spherical configuration). As λ is further increased the thinner hemisphere expands more than the thickened hemisphere and the asphericity grows to the second maximum in Fig. 2. The membrane then returns to the spherical mode at the second bifurcation point.

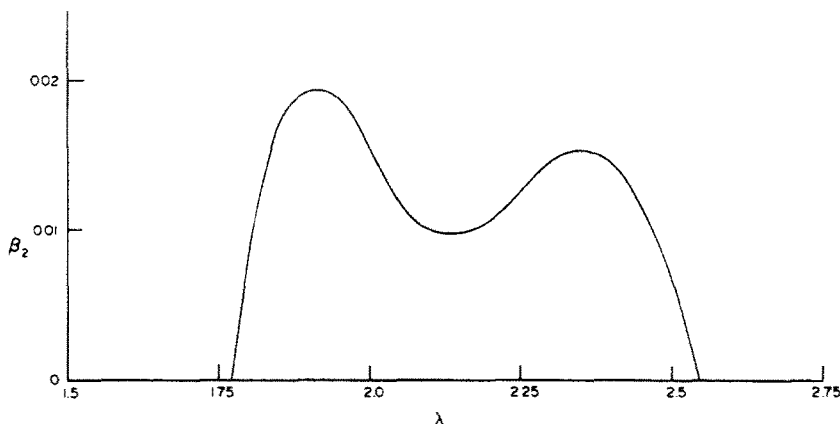


Fig. 2. Plot of the geometrical asphericity β_2 against λ for the three-term strain-energy function (29).

Also of interest is the volume change on going from the spherical to the aspherical configuration. It was shown in [5] that there is no volume change to first order in small displacements. In Fig. 3 we show that this is not so for the developing aspherical mode. We plot the ratio V/V_S against λ for the three-term strain-energy function (29), where V is the enclosed volume in the aspherical configuration and V_S is the volume in the spherical configuration at the same pressure.

We have shown in Fig. 2 that the strain-energy function (29) does not allow a large change in shape, even at the maximum of the asphericity. In the experimental results available [6, 7] the change of shape is considerably more than that predicted by (29). However, the strain-energy function (29) is *not* a model of either of the rubber-like materials used in [6] or [7] and there is insufficient data available to produce a good model of them. Also, we are assuming that the shape of the membrane remains axisymmetric, which may not necessarily be the case.

In the next section we will show that an initial imperfection in the thickness of the membrane can increase the asphericity and give a closer approximation to the experimental results.

To conclude this section we plot the post-bifurcation curve for a simple single-term strain-energy function with $\alpha_1 = 1.5$.

By plotting the measure of the aspherical shape β_2 against λ several interesting features are shown. There is a single bifurcation point at $\lambda = 1.668$. The scale for β_2 has been changed and the aspherical shape can become quite pronounced. Also, we have "turning points" in the aspherical solution path and *aspherical solutions can exist at values of λ before the bifurcation point*. For a given value of the pressure (or λ) there may be one, two or three aspherical solutions, each successive one corresponds to a greater thinning/thickening of the poles.

This particular strain-energy function is not proposed as a realistic material model, the maximum strains after the first turning point become extremely large.

Needleman[3] has plotted similar curves for imperfect spherical membranes with single-term strain-energy functions.

5. INFLATION OF IMPERFECT SPHERICAL MEMBRANES

It was shown in [2] that imperfections in the initial shape of the middle surface of the membrane do not have a significant effect on the solutions obtained for a perfect sphere. We now consider the case where the initial shape of the membrane middle surface is spherical, but where the thickness is non-uniform. This simple case allows us to use the equations and numerical method of the previous section with only a minor modification.

For definiteness we consider two initial imperfections, one which is asymmetric about the equator and one symmetric. We write

$$(a) \quad H = \bar{H}(1 + \delta \cos \theta), \tag{35}$$

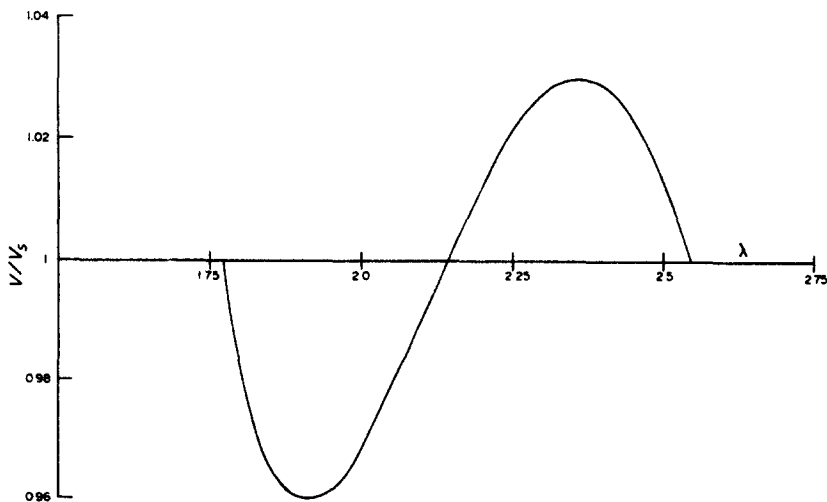


Fig. 3. Plot of the volume ratio V/V_S against λ for the three-term strain-energy function (29).

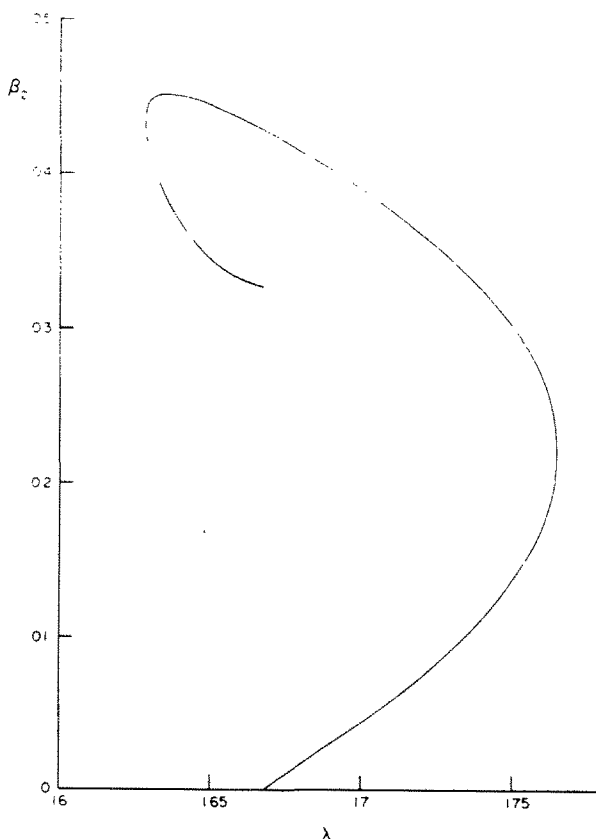


Fig. 4. Plot of the geometrical asphericity β_2 against λ for a single-term strain-energy function with $\alpha_1 = 1.5$.

and

$$(b) \quad H = \bar{H}(1 + \delta \cos 2\theta), \quad (36)$$

where \bar{H} is the average thickness of the membrane and δ is a measure of our imperfection. The smoothness conditions (4) are satisfied by (35) and (36).

To solve eqns (16), (17) and (19) with (13) we again choose the three-term strain-energy function (29) so that the solution paths for the imperfect membranes may be compared with those of a perfect sphere. We write the pressure P^* as

$$P^* = \bar{P}(1 + \delta \cos \Psi), \quad (37)$$

where Ψ is θ or 2θ depending on the choice of (35) or (36). The average pressure \bar{P} is then given by (23) and so we may retain λ as our fundamental parameter. Again for definiteness we choose $\delta = 0.01$, which then represents a maximum thickness variation of about 2%. This is not so large as to be unreasonable, while it is large enough to separate the perfect and imperfect cases.

In Fig. 5 we plot the solution paths, β_2 against λ , for the asymmetric imperfection (35).

It is immediately apparent in Fig. 5 that the bifurcation has been destroyed by the imperfection. The solution initiated in the undeformed configuration corresponds to a greater deformation of the initially thinner pole, as we would expect. The asphericity is greatly increased in the post-bifurcation region and this corresponds to a "perturbation" of the aspherical solution path for a perfect spherical shell, which is also shown. We recall that this aspherical solution path corresponds to *two* equivalent solutions.

Also shown in Fig. 5 is a closed solution path. The upper portion of this closed curve also corresponds to a perturbation of the aspherical solution path for a perfect sphere, but, in this case, the initially thicker pole is deformed much more than the other, initially thinner, pole. The lower portion of this closed solution path is a perturbation of the spherical configuration of an

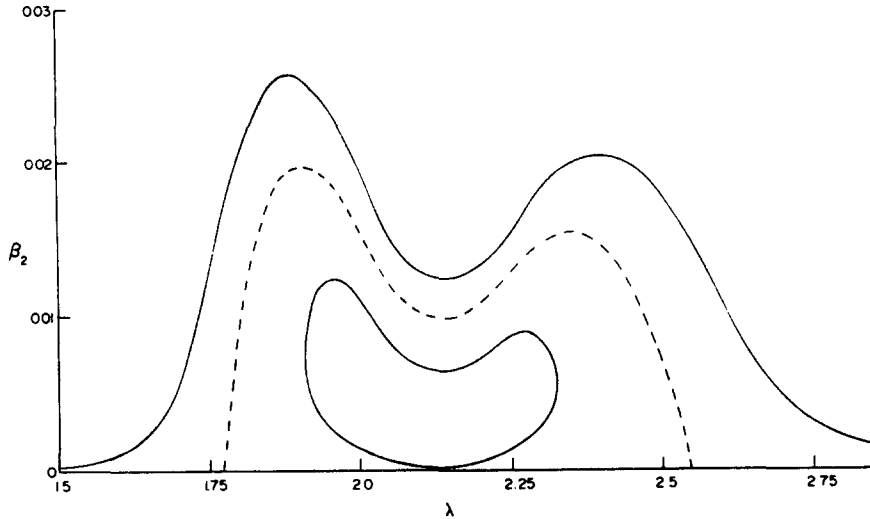


Fig. 5. Plot of the geometrical asphericity β_2 against λ for an asymmetric initial thickness imperfection. The post-bifurcation path for a perfect sphere is included (-----).

initially perfect spherical shell. The initially thicker pole is deformed slightly more than the thinner pole. Clearly this closed solution path may only be reached from the undeformed configuration by "snap through".

Figure 6 shows the corresponding solution curves for the symmetric imperfection (36). In this case the thinning/thickening remains indifferent to the choice of pole and so the two solutions are equivalent. This means that bifurcation can still occur. The fundamental solution (corresponding to the trivial solution in the spherical case) corresponds to a deformation that is symmetric about $\theta = \pi/2$ with the (thinner) equator expanding more than any other radius. The point in the middle of the post-bifurcation range where the post-bifurcation path and the fundamental solution path cross has no special significance. While the asphericity of each solution is the same the two deformations are very different.

Needleman[3] has plotted curves similar to those given here for imperfections of 0.001 and 0.0001 in order to approach the perfectly spherical case. However, the existence of bifurcation points or disjoint solution paths was not mentioned.

6. ASYMPTOTIC SOLUTIONS

In order to obtain some insight into the possible behaviour of post-bifurcation paths we now consider the asymptotic shape of inflated membranes as the enclosed volume $\rightarrow \infty$. By returning to the equations for a general axisymmetric membrane, (10) and (11), we can also consider the asymptotic shape of imperfect membranes.

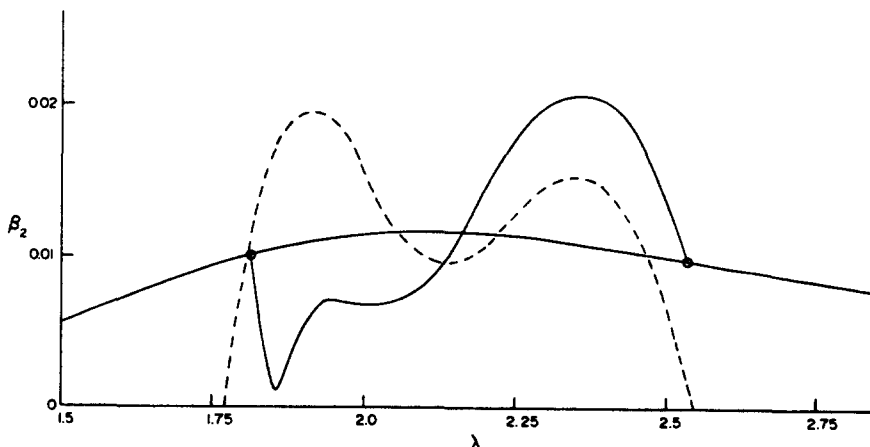


Fig. 6. Plot of the geometrical asphericity β_2 against λ for a symmetric initial thickness imperfection. The bifurcation points are denoted by O. Also included is the post-bifurcation path for a perfect sphere (-----).

Isaacson[9] has considered this problem for the case of a Mooney–Rivlin material (a two-term strain–energy function with $\alpha_1 = 2$, $\alpha_2 = -2$). We extend his analysis to the full class of strain–energy functions (26).

Wu[13] has given a formal asymptotic analysis for the Mooney–Rivlin case, but we do not use his approach here.

From (26) we have

$$\hat{W}_1 = \mu_n(\lambda_1^{\alpha_n} - (\lambda_1\lambda_2)^{-\alpha_n})/\lambda_1, \quad (38)$$

$$\hat{W}_2 = \mu_n(\lambda_2^{\alpha_n} - (\lambda_1\lambda_2)^{-\alpha_n})/\lambda_2. \quad (39)$$

Substituting into (10) and (11) we can write

$$\mu_n(\lambda_1^{\alpha_n} - (\lambda_1\lambda_2)^{-\alpha_n})[2\lambda_1^2 z' + r(r''z' - r'z'')] - \mu_n(\lambda_2^{\alpha_n} - (\lambda_1\lambda_2)^{-\alpha_n})\lambda_1^2 z' = 0, \quad (40)$$

$$2\mu_n(\lambda_1^{\alpha_n} - (\lambda_1\lambda_2)^{-\alpha_n})/\lambda_1^2 \lambda_2 + (r/z')P^* = 0. \quad (41)$$

First suppose that $P \rightarrow \infty$ as the enclosed volume $\rightarrow \infty$ (we suppose that both $\lambda_1(S)$, $\lambda_2(S) \rightarrow \infty$, $S \in [0, L]$). In this case we must have, from (41),

$$\alpha_n > 3 \quad \text{or} \quad \alpha_n < -3/2 \quad \text{at least one } \alpha_n, \quad (42)$$

to ensure the existence of solutions. This is precisely the necessary and sufficient condition to ensure the existence of solutions for all pressures when inflating a *spherical* membrane[10].

The asymptotic shape of the membrane depends on whether the dominant term in the left hand side of (41) corresponds to a positive or negative α_n . We write α^+ for the largest positive α_n and α^- for the negative one of largest magnitude. If there are no positive (negative) α_n 's then $\alpha^+(\alpha^-)$ is taken to be zero.

To satisfy (42) we must have either

$$\alpha^+ > 3 \quad \text{or} \quad \alpha^- < -3/2. \quad (43)$$

Case 1

Suppose that $\alpha^- < -3/2$ and that

$$-2\alpha^- > \alpha^+. \quad (44)$$

In this case (41) becomes

$$2\mu^-/(\lambda_1^{\alpha^-+2}\lambda_2^{\alpha^-+1}) = P^*(r/z') \quad (45)$$

as $P \rightarrow \infty$, where (μ^-, α^-) form a (μ_n, α_n) pair. Equation (40) becomes

$$\mu^-(\lambda_1\lambda_2)^{-\alpha^-}[(r')^2 + (z')^2 + rr'' - r'r''/z'] = 0 \quad (46)$$

which, with (13), is the equation of a sphere[9].

The Mooney–Rivlin strain–energy function ($\alpha^+ = 2$, $\alpha^- = -2$) falls into this category.

Case 2

Now suppose that $\alpha^+ > 3$ and that

$$\alpha^+ > -2\alpha^-. \quad (47)$$

As above, we can show that (40) reduces to

$$\lambda_1^2(1 - (\lambda_2/\lambda_1)^{\alpha^+}) + [(r')^2 + (z')^2 + rr'' - r'r''/z'] = 0 \quad (48)$$

as $P \rightarrow \infty$.

By comparing (48) with (46) we note that the spherical shape is a solution. Generally through, we cannot, at present, rule out other aspherical asymptotic solutions for this subclass of materials. This is also the case when $\alpha^+ = -2\alpha^-$.

If we suppose that

$$-(3/2) < \alpha_n < 3 \quad (\text{each } \alpha_n), \quad (49)$$

then $P \rightarrow 0$ as $\lambda_1, \lambda_2 \rightarrow \infty$ and we find similar asymptotic behaviour according to

$$\alpha^+ \leq -2\alpha^-, \quad (50)$$

as discussed above.

In the special case where $\alpha^+ = 3$ or $\alpha^- = -(3/2)$ then P reaches an asymptote as the enclosed volume $\rightarrow \infty$, but we again have the two cases according to (50).

For a single-term strain-energy function we note that $\alpha_1 < 0$ ensures that the asymptotic shape is a sphere, while this is not necessarily so if $\alpha_1 > 0$.

From (48) and (46) we can see that any possible aspherical asymptotic solutions arise from the term $(\lambda_2/\lambda_1)^\alpha$. From (6) and (7) this term depends on the initial shape of the membrane middle surface through $R(S)$ but not on the initial thickness $H(S)$. *Consequently initial imperfections in the shell thickness do not affect the asymptotic shape.* We have already noted that initial imperfections in shape do not appreciably affect the bifurcation behaviour of spherical membranes. Heuristically it does not seem likely that the initial shape will have much effect on the asymptotic shape. If this is so the spherical configuration will be the *unique* solution to (48).

If a strain-energy function predicts a closed loop bifurcation behaviour (or no bifurcation at all) then there will in general be a unique solution path for a large enough inflation (as indicated by Figs. 5 and 6). In this case the asymptotic shape of both perfect and imperfect shells will be spherical.

However, there is a large class of strain-energy functions ($\alpha^+ > -2\alpha^-$) which *may* allow aspherical asymptotic shapes. For these strain-energy functions which have a pair of bifurcation points we cannot exclude the possibility of two distinct post-bifurcation paths, existing for all values of λ and not returning to the spherical solution path.

Acknowledgements—The author would like to thank Dr. R. W. Ogden for helpful comments on an early draft of this work, which was supported by a Science Research Council Research Grant.

REFERENCES

1. V. I. Feodos'ev, On equilibrium modes of a rubber spherical shell under internal pressure. *PMM* **32**, 339 (1968).
2. A. Needleman, Necking of spherical membranes. *J. Mech. Phys. Solids* **24**, 339 (1976).
3. A. Needleman, Inflation of spherical rubber balloons. *Int. J. Solids Structures* **13**, 409 (1977).
4. D. M. Haughton and R. W. Ogden, On the incremental equations in non-linear elasticity—I. Membrane theory. *J. Mech. Phys. Solids* **26**, 93 (1978).
5. D. M. Haughton and R. W. Ogden, On the incremental equations in non-linear elasticity—II. Bifurcation of pressurized spherical shells. *J. Mech. Phys. Solids* **26**, 111 (1978).
6. M. J. Sewell, Some mechanical examples of catastrophe theory. *Bull. Inst. Math. Appl.* **12**, 163 (1976).
7. H. Alexander, Tensile instability of initially spherical balloons. *Int. J. Engng Sci.* **9**, 151 (1971).
8. R. W. Ogden, Large deformation isotropic elasticity—on the correlation of theory and experiment for incompressible rubberlike solids. *Proc. R. Soc. Lond. A.* **326**, 565 (1972).
9. E. Isaacson, The shape of a balloon. *Commun. Pure Appl. Math.* **18**, 163 (1965).
10. D. M. Haughton, Bifurcation of spherical and cylindrical shells at finite deformation. Ph.D Thesis, University of Bath (1979).
11. A. E. Green and J. E. Adkins, *Large elastic deformations*. Oxford University Press (1970).
12. D. M. Haughton and R. W. Ogden, Bifurcation of inflated circular cylinders of elastic material under axial loading—I. Membrane theory for thin-walled tubes. *J. Mech. Phys. Solids* **27**, 179 (1979).
13. C. H. Wu, Spherelike deformations of a balloon. *Quart. Appl. Math.* **30**, 183 (1972).